AFRL-VA-WP-TP-2002-326

A METHOD FOR THE DETERMINATION OF THE ATTAINABLE MOMENT SET FOR NON-LINEAR CONTROL EFFECTORS

Michael A. Bolender
David B. Doman

OCTOBER 2002

Approved for public release; distribution is unlimited.

AIR VEHICLES DIRECTORATE
AIR FORCE RESEARCH LABORATORY
AIR FORCE MATERIEL COMMAND
WRIGHT-PATTERSON AIR FORCE BASE, OH 45433-7542

REPORT DOCUMENTATION PAGE

Form Approved
OMB No. 0704-0188

1. REPORT DATE *(DD-MM-YY)*	2. REPORT TYPE	3. DATES COVERED *(From - To)*
October 2002	Conference Paper Preprint	

4. TITLE AND SUBTITLE

A METHOD FOR THE DETERMINATION OF THE ATTAINABLE MOMENT SET FOR NON-LINEAR CONTROL EFFECTORS

5a. CONTRACT NUMBER
IN-HOUSE

5b. GRANT NUMBER

5c. PROGRAM ELEMENT NUMBER
N/A

6. AUTHOR(S)
Michael A. Bolender
David B. Doman

5d. PROJECT NUMBER
N/A

5e. TASK NUMBER
N/A

5f. WORK UNIT NUMBER
N/A

7. PERFORMING ORGANIZATION NAME(S) AND ADDRESS(ES)
Control Theory Optimization Branch (AFRL/VACA)
Control Sciences Division
Air Vehicles Directorate
Air Force Research Laboratory, Air Force Materiel Command
Wright-Patterson Air Force Base, OH 45433-7542

8. PERFORMING ORGANIZATION REPORT NUMBER
AFRL-VA-WP-TP-2002-326

9. SPONSORING/MONITORING AGENCY NAME(S) AND ADDRESS(ES)
Air Vehicles Directorate
Air Force Research Laboratory
Air Force Materiel Command
Wright-Patterson Air Force Base, OH 45433-7542

10. SPONSORING/MONITORING AGENCY ACRONYM(S)
AFRL/VACA

11. SPONSORING/MONITORING AGENCY REPORT NUMBER(S)
AFRL-VA-WP-TP-2002-326

12. DISTRIBUTION/AVAILABILITY STATEMENT
Approved for public release; distribution is unlimited.

13. SUPPLEMENTARY NOTES
Submitted for publication for IEEE Aerospace Conference presentation, Big Sky, MT, 3/17/03.

14. ABSTRACT *(Maximum 200 Words)*
A method for generating the attainable moment set for a class of multiple non-linear control effectors is presented. The Jacobian Rank Deficiency Criteria from Swept Volume Theory is used to determine a set of control effector positions that in turn determine a set of candidate surfaces that comprise the boundary of the attainable moment set.

15. SUBJECT TERMS

16. SECURITY CLASSIFICATION OF:			17. LIMITATION OF ABSTRACT:	18. NUMBER OF PAGES	19a. NAME OF RESPONSIBLE PERSON (Monitor)
a. REPORT	b. ABSTRACT	c. THIS PAGE			David Doman
Unclassified	Unclassified	Unclassified	SAR	16	19b. TELEPHONE NUMBER *(Include Area Code)* (937) 255-8451

A Method for the Determination of the Attainable Moment Set for Non-Linear Control Effectors

Michael A. Bolender
David B. Doman
Air Force Research Laboratory
Control Theory and Optimization Branch
2210 Eighth Street
Wright-Patterson AFB, OH 45433, USA
937-255-8492/937-255-8451
Michael.Bolender@wpafb.af.mil
David.Doman@wpafb.af.mil

Abstract—A method for generating the attainable moment set for a class of multiple non-linear control effectors is presented. The Jacobian Rank Deficiency Criteria from Swept Volume Theory is used to determine a set of control effector positions that in turn determine a set of candidate surfaces that comprise the boundary of the attainable moment set. The first order necessary conditions are derived for a point to be on the boundary by considering a non-linear programming problem. An algorithm is given where the Kuhn-Tucker points for a given point in the pitch-roll plane are constructed for each control effector configuration that forms a candidate boundary. The Kuhn-Tucker points are then checked for feasibility, and the points on the boundary are the ones that maximize and minimize the objective function. This method is computationally efficient despite the fact that a large set of points in is searched since the evaluation of the Kuhn-Tucker points is straight forward and less computationally intensive than those methods which require an exhaustive search over every point on each candidate surface.

TABLE OF CONTENTS

1. INTRODUCTION

Concepts for future aerospace vehicles often have redundant control effectors in order to optimize vehicle performance and to make the aircraft more robust to potential failures. One such example is the X-33, which has eight control surfaces that are capable of being actuated independently. Because the X-33 is unlike traditional aircraft, which have only a single control effector controlling the vehicle's attitude about one axis, the relationship between control effector and control axis is not "one-to-one." Therefore, whenever the number of effectors exceeds the number of axes being controlled, allocating control effectors is necessary to achieve the desired vehicle response.

Numerous control allocation and control effector mixing algorithms have been developed over the past decade and excellent survey papers have been written that point out the strengths and weaknesses of the existing approaches [1]. These control mixing and control allocation algorithms are capable of dealing with systems where the moments are linearly related to control effector positions and have the ability to account for constraints on those positions. Some of these algorithms generate constrained control effector commands that ensure that the effectors are never driven beyond their physical limits. Most of the algorithms, however, assume that linear relationships exist between the pseudo-commands (i.e., controlled variable commands) and the effector positions. While this assumption is at least locally valid for many of the control surfaces found on aircraft, there are exceptions.

One particular case where this assumption can result in incorrect control surface deflections and return unnecessarily conservative results involves the use of left-right aerodynamic control surfaces on aircraft. Examples of left-right aerodynamic surfaces include left-right elevators and left-right ailerons. This type of surface can generally produce pitching, rolling and yawing moments. While these surfaces normally produce pitching and rolling moments that are locally linear in control surface deflection, they can have a highly nonlinear contribution to the yawing moment especially when parasitic drag dominates induced drag effects.

In particular, these surfaces can generate yawing moments that are of the same sign whether they are de-

IEEEAC paper # 1192

component of acceleration normal to the surface and the acceleration along the principal normal." The acceleration parameter defined in Reference [6] is

$$\eta = a_n - \kappa v^2 \tag{19}$$

where a_n is the projection of the acceleration on the unit normal at a given point on a candidate surface, and κv^2 is the normal acceleration, as would be defined in the Frenet-Serret coordinate frame. While the principal normal is directed towards the instantaneous center of curvature for a curve in $\mathbb{R}^3$, the definition of the principal normal for a point on a surface is ambiguous since it depends upon the path that the particle is moving. Nevertheless, the authors of Reference [6] show using differential geometry that if the particle is indeed travelling on a surface that is a boundary, then η, which is a quadratic form, will be either positive or negative semi-definite. This result is further augmented with an additional condition that must be met if one or more of the parameters is set at an upper or lower bound. The derivation and the algorithm for computing the quadratic form, η, can be found in Reference [6].

An New Method for the Determination of the AMS Volume

As stated previously, the composite AMS is generated by translating the origin of the AMS for one left-right pair to every point on the AMS for the second left-right pair. We also know, from using the Jacobian rank deficiency criteria, the set of control surface deflections that will generate the candidate surfaces for the AMS boundary.

In this section, we will address the approach of Doman and Sparks and show how to extend it to the problem of computing the AMS for all three axes. The theorem developed independently by Doman and Sparks and found in Reference [3] gives a necessary condition for a point to lie on the composite boundary. Simply stated, for a composite function that is the sum of two functions,

$$h(x, \bar{x}) = f(\bar{x}) + g(x - \bar{x}) \tag{20}$$

the necessary condition for a point to be on the boundary of the composite function is

$$\frac{\partial}{\partial(x-\bar{x})} g(x-\bar{x})\Big|_{x=\bar{x}^*} = \frac{\partial}{\partial \bar{x}} f(\bar{x})\Big|_{x=\bar{x}^*} \tag{21}$$

The proof is omitted here but can be found in Reference [3]. It is important to note that there is no restriction on the dimension of x. Therefore, for any fixed value of x, we can determine the optimum value of $\bar{x}$ where $g(x-\bar{x})$ attaches to $f(\bar{x})$ in order to maximize or minimize $h(x, \bar{x})$.

In order to apply the above necessary condition to the determination of the composite AMS, two additional lemmas are needed in order to account for the fact that there are bounds on the variables $x - \bar{x}$ and $\bar{x}$, which in turn set limits on their respective functions. The lemmas are repeated here for completeness:

Lemma 1: If $(x - \bar{x}^*) \geq x_{max_g}$ then the boundary point is given by $P[\bar{x}^* + x_{max_g}, h(x_{max_g}, \bar{x}^*)]$

Lemma 2: If $(x - \bar{x}^*) \leq x_{min_g}$ then the boundary point is given by $P[\bar{x}^* + x_{min_g}, h(x_{min_g}, \bar{x}^*)]$

Doman and Sparks successfully implemented their approach and were able to determine the AMS boundary for the case where the rolling moment was a linear function of the control displacement and the yawing moment was a second order function of control surface displacement, as shown in Figure 1. It is important to note that the result that was achieved was *not* for the case where the pitching moment was constrained to zero. Instead, their composite AMS was a projection of the AMS volume onto the roll-yaw plane. The question of how to apply the above result to the determination of the AMS *volume* still remained.

We know from the Jacobian rank deficiency criteria that we have to consider all combinations of pairs of control effectors set at their upper and lower limits. In addition, there are four additional singular surfaces that arise from the reduced order Jacobians. What we present here is an outline of how to determine the boundary of the AMS when given any point in the L-M plane. For purposes of illustration, we will only combinations of δ_2 and δ_4 set at their position limits. In actuality, all the control surface deflections that are in the set S must be evaluated. The minimum (or maximum) yawing moment is determined by forming and searching an array of yawing moments generated by all the pairs in the set S for a given point (L, M).

Begin by considering the moment equations for the 1-2 pair.

$$L_{12} = K_l(\delta_1 - \delta_2) \tag{22}$$

$$M_{12} = K_m(\delta_1 + \delta_2) \tag{23}$$

$$N_{12} = K_n(\delta_1^2 - \delta_2^2) \tag{24}$$

where K_l, K_m, K_n are the rolling, pitching, and yawing control derivatives respectively. Eliminating the parameter δ_1, we can write the pitching and yawing moments as functions of the rolling moment.

$$M_{12}(L_{12}) = K_m(2\delta_2 + \frac{L_{12}}{K_l}) \tag{25}$$

$$N_{12}(L_{12}) = K_n(\frac{L_{12}^2}{K_l^2} + 2\frac{L_{12}\delta_2}{K_l}) \tag{26}$$

Repeating the process for the 3-4 effector pair to elimi-

nate δ_3 subsequently yields

$$M_{34}(L_{34}) = C_m(2\delta_4 + \frac{L_{34}}{C_l}) \tag{27}$$

$$N_{34}(L_{34}) = C_n(\frac{L_{34}^2}{C_l^2} + 2\delta_4\frac{L_{34}}{C_l}) \tag{28}$$

where C_l, C_m, and C_n are the rolling, pitching, and yawing control derivatives respectively.

In order to compute the AMS volume, we will assume that all ordered pairs (L, M) can be computed *a priori*. We fix L and M at some arbitrary value and let $L_{34} = L - \bar{L}$ (the choice of notation here is to be consistent with Reference [3]). The equations for the pitching and yawing moments then become

$$M = K_m(2\delta_2 + \frac{\bar{L}}{K_l}) + C_m(2\delta_4 + \frac{L-\bar{L}}{C_l}) \tag{29}$$

$$N = K_n(\frac{\bar{L}^2}{K_l^2} + 2\frac{\bar{L}\delta_2}{K_l}) + C_n(\frac{(L-\bar{L})^2}{C_l^2} + 2\frac{(L-\bar{L})\delta_4}{C_l}) \tag{30}$$

If we were not concerned with the pitching moment, we would simply apply the theorem in Reference [3] and differentiate Equation 30 and solve for the attaching point, $\bar{L}$. Because we are including an additional equation for the pitching moment, an equality constraint must be added to our objective function. Furthermore, since δ_2 or $\delta_4$ha ve physical limits, these constraints must be included in the objective function as inequality constraints. The downside is that we must now solve a non-linear programming problem with a single equality constraint and four inequality constraints in order to find the boundary that encloses the AMS. By including the inequality constraints for control effectors, we no longer have to carry along Lemmas 1 and 2 as they are now accounted for in the objective function. We form the following Lagrangian by augmenting Equation 30 with the equality and inequality constraints:

$$\begin{aligned}\mathscr{L} = {} & K_n\left(\frac{\bar{L}^2}{K_l^2} + 2\frac{\bar{L}\delta_2}{K_l}\right) + C_n\left(\frac{(L-\bar{L})^2}{C_l^2} + 2\frac{(L-\bar{L})\delta_4}{C_l}\right) \\ & - \lambda\left(M - K_m\left(2\delta_2 + \frac{\bar{L}}{K_l}\right) - C_m\left(2\delta_4 + \frac{(L-\bar{L})}{C_l}\right)\right) \\ & - u_1(\bar{\delta}_2 - \delta_2) - u_2(\delta_2 - \underline{\delta}_2) - u_3(\bar{\delta}_4 - \delta_4) - u_4(\delta_4 - \underline{\delta}_4)\end{aligned} \tag{31}$$

Differentiating the Lagrangian with respect to $\bar{L}$, δ_2, δ_4, and λ gives the first order necessary conditions:

$$\begin{aligned}\frac{\partial\mathscr{L}}{\partial\bar{L}} = {} & 2\frac{K_n}{K_l^2}\left(\bar{L} + K_l\delta_2\right) + 2\frac{C_n}{C_l^2}\left(L - \bar{L} + C_l\delta_4\right) \\ & - \lambda\left(\frac{C_m}{C_l} - \frac{K_m}{K_l}\right).\end{aligned} \tag{32}$$

$$\frac{\partial\mathscr{L}}{\partial\delta_2} = 2\frac{K_n}{K_l}\bar{L} + 2\lambda K_m + u_1 - u_2 \tag{33}$$

$$\frac{\partial\mathscr{L}}{\partial\delta_4} = 2\frac{C_n}{C_l}\left(L - \bar{L}\right) + 2\lambda C_m + u_3 - u_4 \tag{34}$$

$$\frac{\partial\mathscr{L}}{\partial\lambda} = M - K_m(2\delta_2 + \frac{\bar{L}}{K_l}) - C_m\left(2\delta_4 + \frac{L-\bar{L}}{C_l}\right) \tag{35}$$

Setting Equations 32-35 equal to zero and solving for $\bar{L}$, δ_2, δ_4, and λ yields

$$\bar{L} = \frac{K_l(2C_nK_mL + C_lC_mu_2 - C_lK_mu_4)}{2(C_nK_lK_m + C_lC_mK_n)} \tag{36}$$

$$\delta_2 = \frac{-2C_nK_mL + 2C_nK_lM - 2C_lu_2 + u_4(C_mK_l + C_lK_m)}{4(C_nK_lK_m + C_lC_mK_n)} \tag{37}$$

$$\delta_4 = \frac{-2C_mK_nL + 2C_lK_nM + u_2(C_mK_l + C_lK_m) - 2K_lK_mu_4}{4(C_nK_lK_m + C_lC_mK_n)} \tag{38}$$

$$\lambda = \frac{-2C_nK_nL + C_nK_lu_2 + C_lK_nu_4}{2(C_nK_lK_m + C_lC_mK_n)} \tag{39}$$

When solving the optimization problem, we must also consider the following equality and inequality constraints:

$$u_1(\bar{\delta}_2 - \delta_2) = 0 \tag{40}$$

$$u_2(\delta_2 - \underline{\delta}_2) = 0 \tag{41}$$

$$u_3(\bar{\delta}_4 - \delta_4) = 0 \tag{42}$$

$$u_4(\delta_4 - \underline{\delta}_4) = 0 \tag{43}$$

$$u_1, u_2, u_3, u_4 \geq 0 \tag{44}$$

We must evaluate all the possible combinations of δ_2 and δ_4 taken one at time and two at a time. This will result in eight different Kuhn-Tucker points to consider. If all the inequality and equality constraints are satisfied, only then is the Kuhn-Tucker point considered as a feasible solution. A tally of the feasible Kuhn-Tucker points is kept until all the surfaces defined by the points in S are searched for feasible Kuhn-Tucker points for the given values of L and M. Once the tally is completed, then the minimum value of N can be found. It is this value which lies on the boundary of the AMS. Note that it is possible for there to be multiple sets of control surface deflections that will produce the same point on the boundary.

For example, we take the control derivatives to have the following values: K_l = 4610 ft-lb/deg, K_m =

flected up or down. This is because they generate a drag force on the side of the vehicle on which they are located regardless of whether they deflected in the positive or negative direction. The yawing moments generated by these effectors are usually small when compared to a primary yaw-axis effector like a rudder; however, their effects can become significant when a rudder fails or when the aircraft is operating at high angles of attack where flow over the rudder is interrupted by the body.

This particular nonlinearity is used as motivation and serves as an example for the methods explored in this paper. Methods for generating an attainable moment set for a class of multiple non-linear effectors are presented.

2. Attainable Moment Set for a Single Left-Right Pair

Durham [2] developed and subsequently refined methods for determining attainable moment sets (AMS) for effectors that generate moments $\boldsymbol{M}$ that are linear functions $\boldsymbol{M} = \boldsymbol{B\delta}$ of the effector positions $\boldsymbol{\delta}$ subject to constraints on those positions $\boldsymbol{\delta} = \{\delta | \delta \in [\underline{\delta}, \bar{\delta}]\}$. The general solution to finding the attainable moment set for an over-actuated linear system with position constraints involves constructing a polyhedron in moment space. Potential vertices are constructed by locking all control effectors at their extreme positions in all possible combinations while allowing two effectors to traverse the range of their possible positions. Durham's algorithm connected the vertices to form potential boundary facets and determined which facets were on the boundary of the AMS.

Left-right (LR) pairs of effectors such as ailerons, elevators and flaps, generate non-linear contributions to the vehicle yawing moment. Figure 1 shows the yawing moment that is generated by deflecting the right elevon of a particular lifting body vehicle. One can see that a parabolic fit provides an adequate approximation of the original data. Generation of linear fits to this data for use in a conventional control allocator that assume a linear relationship between the moments and control effector deflections is problematic. This is because lines fitted using either negative deflection or positive deflection data results in lines with slopes of opposite signs. Furthermore, since no single line can accurately model the data and no matter which line is selected, the sign of the yawing moment estimate will be incorrect half of the time.

Here we examine a case where a LR pair of elevons exerts a yawing moment N that is proportional to the square of deflection and rolling and pitching moments L and M

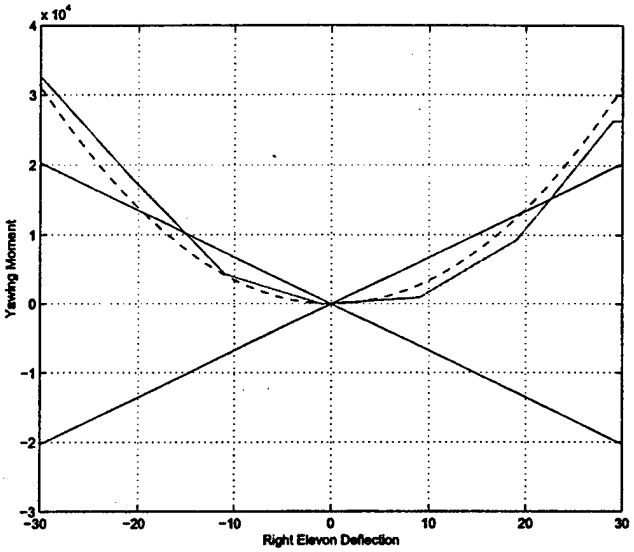

Figure 1. Yawing Moment due to Right Elevon Deflection

that are linear functions of deflection

$$L = L_{le}\delta_{le} + L_{re}\delta_{re} \quad (1)$$

$$M = M_{le}\delta_{le} + M_{re}\delta_{re} \quad (2)$$

$$N = N_{le^2}\delta_{le}^2 + N_{re^2}\delta_{re}^2 \quad (3)$$

From the curve fits to aerodynamic data for a lifting body model at a subsonic flight condition, we select $N_{re^2} = -N_{le^2} = 34$ ft-lb/deg^2 and $L_{re} = -L_{le} = -4610$ ft-lb/deg, and $M_{le} = M_{re} = -2489$ ft-lb/deg. The AMS is generated by holding each control surface at a fixed deflection while allowing the other surface to vary over its range of possible values and is shown in Figure 6. Note in particular that the shape of the AMS is hyperbolic paraboloid. This saddle shape is a characteristic of left-right pairs on any aircraft.

The AMS is also shown in Figure 3 for the yawing moment as a linear function of the deflections. For the linear approximation we fit data over half of the range of deflections to obtain $N_{le} = -N_{re} = \pm 676$ ft-lb/deg. The sign ambiguity results from the yawing moment derivatives' dependency on the sign of the deflections; either choice of sign will only yield a yawing moment with the correct sign over half of the deflection range. The AMS for the linear case shows that a control allocator that incorrectly assumes a linear relationship between the yawing moment and the effector deflections will be constrained to rolling, pitching, and yawing moments that lie on a plane in moment space. The AMS for the improved effector model (Figure 2) shows that larger regions in the roll-yaw plane are reachable and the intersection of lines of constant effector deflection define the proper blend of effectors required to achieve a particular rolling , pitching, and yawing moment that lies within the AMS.

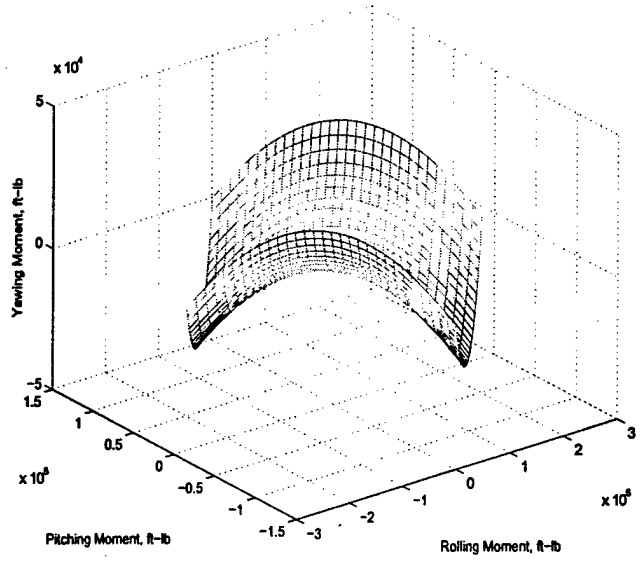

Figure 2. Nonlinear AMS and Lines of Constant Deflection in Moment Space

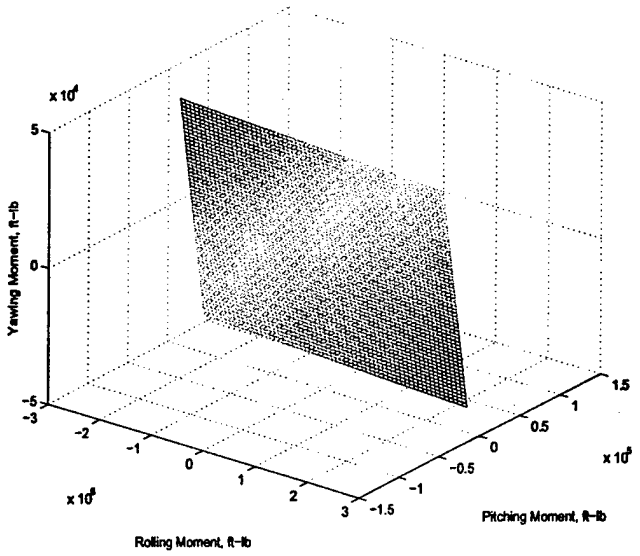

Figure 3. Linear AMS for a Single Left-Right Pair

3. Determination of the Composite AMS for Multiple Effectors

The generation of an AMS for a single LR pair is relatively straightforward. Here we would like to explore methods for generating the AMS for multiple LR effector pairs. To consider how this might be accomplished we consider the rolling, pitching, and yawing moments that can be generated by two LR effector pairs of the form

$$L = L_1\delta_1 + L_2\delta_2 + L_3\delta_3 + L_4\delta_4 \quad (4)$$

$$M = M_1\delta_1 + M_2\delta_2 + M_3\delta_3 + M_4\delta_4 \quad (5)$$

$$N = N_1\delta_1^2 + N_2\delta_2^2 + N_3\delta_3^2 + N_4\delta_4^2 \quad (6)$$

Since there is no aerodynamic coupling between the control effectors, Equations 4-6 can be written as follows:

$$L = L_{12} + L_{34} \quad (7)$$

$$M = M_{12} + M_{34} \quad (8)$$

$$N = N_{12} + N_{34} \quad (9)$$

Therefore, the composite AMS may be generated by placing the origin of the AMS for one left-right pair at each point on the AMS of the other left-right pair. This approach is sufficient for generating every attainable moment; however, a criteria is needed to determine the boundary of the AMS. We will explore the possibility of using swept volume theory to construct the AMS, but due to the fact that the methods for evaluating the boundary are exhaustive searches over each candidate surface, we will present another method that extends the work put forth in Reference [3] that is more computationally efficient.

Swept Volume Theory

Swept Volume Theory is a field of study of that encompasses engineering, mathematics, and computer science and is concerned with the computation and visualization of complex geometric shapes. A swept volume is defined in Reference [4] as "the volume generated by the motion of an arbitrary object along an arbitrary path (or even a surface) possibly with arbitrary rotations." Swept volume theory has applications ranging from robotics to computer aided manufacturing to human factors. In the area of robotics, swept volume theory is used to analyze the workspace to ensure that conflicts between robotic arms can be avoided. For computer aided manufacturing, swept volume theory is used to determine the amount of material a tool removes as it moves along a surface in numerically controlled machining. More applications of Swept Volume Theory can be found in the survey paper by Abdel-Malek, Blackmore, and Joy [4]. The formalism of swept volume theory is presented here because of the recognition that the sweeping of one AMS for a first pair of left-right control effectors over the AMS for a second left-right pair will generate the composite AMS.

Let us begin by considering some arbitrary object that is defined by the parametric equation $\Gamma(\boldsymbol{u})$. This object is swept along a curve or surface that is parameterized by $\Psi(\boldsymbol{v})$. Furthermore, the rotation matrix, $R(\boldsymbol{v})$ defines the orientation of the object at every point on the trajectory defined by $\Psi(\boldsymbol{v})$. The Swept Volume is then defined as

$$\xi(q) = R(v)\Gamma(u) + \Psi(v) \quad (10)$$

where $q^T = [u_1\ u_2\ \ldots\ u_m\ v_1\ v_2\ \ldots\ v_n]$ is the extended vector of length $m+n$. Furthermore, it is assumed that each of the parameters q_i are bounded from above and below $\underline{q}_i \leq q_i \leq \bar{q}_i$. Note that $\xi(q)$ describes the entire set of accessible points in the swept volume. In general,

the system of equations given by Equation 10 will only be square if the body is being swept along a curve. In the more general case of sweeping along a surface, we are dealing with an underdetermined set of non-linear equations.

If we consider a fixed vector, q_0, and we linearize Equation 10 about this point, we get

$$\Delta\xi(q) = \xi(q_0) + J(q_0)(q - q_0) + \mathcal{O}(h) \qquad (11)$$

where $J = [\partial\xi_i/\partial q_i]$ is the $3 \times (n+m)$ Jacobian Matrix for Equation 10. Singularity of the Jacobian implies that the sweep equation (Equation 10) is a local maximum or minimum for some set of values. In the case where the trajectory is simply a curve, determining the singular points of the Jacobian is rather straight-forward. Abdel-Malek and Yeh [5] generalized the result to higher dimension trajectories, and they further show that there are three conditions under which the Jacobian becomes singular. These conditions in turn can be specified in terms of the rank deficiency of the Jacobian and subsequently will generate the candidate surfaces for the boundary of the swept volume. The three criteria that are outlined in Reference [5] are

1. The rank-deficiency singularity set
2. The rank-deficiency of the reduced-order accessible set
3. Constraint Singularities.

The rank-deficiency singularity set in Item 1 is determined by considering the $n+m$ combinations of the columns of J that will make it a 3×3 matrix. The determinant of each sub-matrix is then computed, and the $n+m$ equations are solved simultaneously for those values of q which will render the Jacobian singular. This set of points is denoted as $S_1 = \{\tilde{\mathbf{q}} \in \mathbb{R}^n | \dim \mathrm{Null} J(\mathbf{q}) \geq 1\}$.

In Item 2, a reduced-order set of equations is formed by taking one of the generalized parameters, q_i, and setting it at one of its limits in Equation 10. A new Jacobian, or subset of Jacobians if $n+m > 4$, J_R, is then found for the reduced-order equations. The determinant of the new Jacobian is then computed and solved for those values which cause the reduced-order Jacobian to be singular. This is repeated considering each q_i alone until all of the reduced-order Jacobians have been examined with each of the $n+m$ parameters set at their upper and lower bounds. We now have a second set of singular points that we will denote as $S_2 = \{\tilde{\mathbf{q}} \in \mathbb{R}^n | \dim \mathrm{Null} J_R(\mathbf{q}) \geq 1\}$.

In Item 3 it is recognized that a boundary is reached when all but 2 of the generalized parameters, q_i, are set to one of their limits. By enforcing $n+m-2$ constraints to be active and varying the two free parameters over their allowable range, surfaces are generated which are embedded in $\mathbb{R}^3$. Although these surfaces don't necessarily cause a rank-deficiency condition, they nevertheless must be evaluated in order to determine whether they are on the boundary (note the similarity with Durham's [2] approach for the construction of the linear AMS.) There will be a total of $2(n+m)(n+m-1)$ surfaces resulting from the application of the parameter constraints. For the case that we will consider where we have $n+m=4$, we will have 24 candidate surfaces. The final set of points to consider as candidates for the boundary of the swept volume is $S_3 = \{\tilde{q} \in \mathbb{R}^n | q_i = q_i^{lim} \text{ and } q_j = q_j^{lim}, i \neq j\}$ where q_i^{lim} is either the upper or lower limit for q_i.

The set $S = S_1 \cup S_2 \cup S_3$ defines the set of surfaces that are candidates for the boundary of the swept volume. While the determination of the candidate surfaces is a rather straight-forward procedure, determining whether a surface, or even an area of the surface is on the swept volume boundary is non-trivial. In fact, this is an area of active research within in the swept volume community. We will then outline a few approaches and discuss the difficulty with their implementation.

Application of Swept Volume Theory—The moment equations, as they are stated in Equations 4 - 6, fit naturally into the framework of Equation 10. We define $\Psi(v) = [K_l(\delta_1 - \delta_2)\ K_m(\delta_1 + \delta_2)\ K_n(\delta_1^2 - \delta_2^2)]^T$ and $\Gamma(u) = [C_l(\delta_3 - \delta_4)\ C_m(\delta_3 + \delta_4)\ C_n(\delta_3^2 - \delta_4^2)]^T$. Since we are only concerned with a pure translation of $\Gamma(u)$ over $\Psi(v)$, the rotation matrix, $R(v)$, then becomes the identity matrix, I_3. We form the Jacobian for the sweep equation

$$J = \begin{bmatrix} K_l & -K_l & C_l & -C_l \\ K_m & K_m & C_m & C_m \\ 2K_n\delta_1 & -2K_n\delta_2 & 2C_n\delta_3 & -2C_n\delta_4 \end{bmatrix}. \qquad (12)$$

To begin finding the points defined is S_1, we need to examine the four determinants where the Jacobian is square. The Jacobian is made square by eliminating one of the four columns. We then get the following four determinants that are to be solved simultaneously for the δ_i:

$$|J_1| = -2K_m(-2C_n\delta_3K_l + K_n(C_l(\delta_1+\delta_2) + (\delta_1-\delta_2)K_l)) \qquad (13)$$

$$|J_2| = 2K_m(-2C_n\delta_4K_l + K_n(C_l(\delta_1+\delta_2) + (-\delta_1+\delta_2)K_l)) \qquad (14)$$

$$|J_3| = -2K_m(C_nK_l(\delta_3+\delta_4) + C_l(C_n(\delta_3-\delta_4) - 2\delta_1K_n)) \qquad (15)$$

$$|J_4| = 2K_m(C_nK_l(\delta_3+\delta_4) + C_l(C_n(-\delta_3+\delta_4) - 2\delta_2K_n)). \qquad (16)$$

There is no solution for this set of equations; therefore, the set $S_1$is the empty set $\{\varnothing\}$. To compute the set of points for the reduced-order set, we need to select one control and set it at either its upper or lower limit in

Equation 10 while allowing the other controls to remain free, and then compute the new Jacobian and its determinant. We repeat this procedure for the same control at its other limit, and also for all the other remaining controls. The result of this will be the four determinants in Equations 13-16. The fact that the determinants for the set S_2 are the same as those for the set S_1 is a result of the moment equations being linear in pitch and roll and quadratic in yaw. We now consider each of the determinants individually, and determine the set of points for which there are roots. For example, if we take $\delta_1$to be at its upper limit, we get Equation 16, and solve for δ_2a s a function of δ_3 and δ_4. We then get

$$\delta_2 = \frac{C_n(C_m K_l(\delta_3 + \delta_4) - C_l K_m(\delta_3 - \delta_4))}{2C_l C_m K_n} \qquad (17)$$

The candidate surface that results from substituting Equation 17 into Equations 4-6 is shown in Figure 4. Note that there will only be three additional surfaces

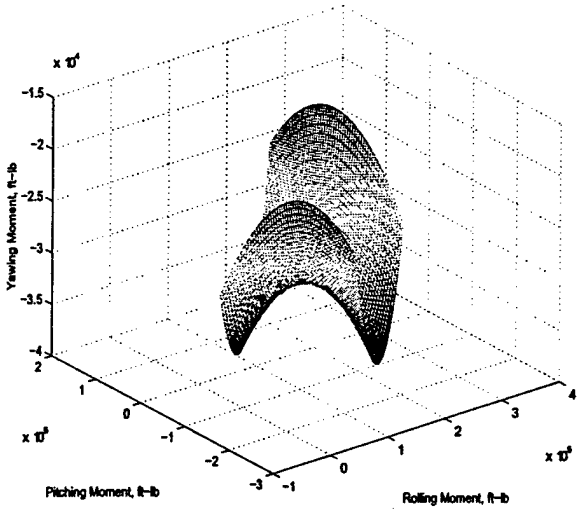

Figure 4. Candidate Surface for the AMS Boundary

that are candidates for the AMS boundary. Because there is only one control effector that appears in any one column of the Jacobian matrix, the determinant is the same for regardless of the whether the control effector is at its upper or lower limit. Also, care must be taken to ensure that the dependent variable (δ_2 in the case above) remains within its position limits. This may result in the independent variables being constrained to an interval that is a subset of the one defined by its upper and lower limits.

The last step is to set two of the control surfaces at their limits and to allow the other two to remain free. This is repeated until for all combinations of controls set at their limits, resulting in 24 more surfaces that are candidates.

Determination of the Swept Volume Boundary—The determination of the swept volume boundary is a challenging problem that remains open [4]. There is no generally accepted method that will allow for the easy identification of the boundary. In this section we will discuss attempts to implement, among other things, a perturbation technique as well as a technique based on the calculation of the "normal acceleration" on each candidate surface.

Consider a candidate surface, $z = f(\delta)$ where $\delta = \{\delta | \delta \in [\underline{\delta}, \bar{\delta}]\}$. Let $\hat{n}(\delta_0)$ be the unit normal to the surface at point δ_0 and $\hat{n}_z(\delta_0)$ be the projection of the unit normal on the z-axis. We now form the equation

$$f(\delta) = f(\delta_0) \pm \epsilon \hat{n}_z. \qquad (18)$$

where ϵ is some small number. The rationale behind Equation 18 is that if a point δ_0 lies on the boundary of the swept volume (or AMS), then there will only be one solution to Equation 18, which will correspond to the solution internal to the volume. Conversely, if the point δ_0 is internal to the volume, there will be two solutions to Equation 18, both internal to the volume. In Reference [5], Abdel-Malek and Yeh claim that using the perturbation equation alone is not sufficient, and that this approach works best when used in conjunction with a method that finds the intersections of all the candidate surfaces. This is needed to remove any ambiguity. In any case, Equation 18 needs to be solved for every point on the candidate surface. Since we are dealing with an underdetermined set of equations in this instance, a numerical root finding technique must be employed to determine the solutions to Equation 18. The pitfall here is that a numerical root finding algorithm will tend to find the root nearest to the initial guess. In general, there may be multiple solutions, both feasible and non-feasible, to each root finding problem. It has been observed that there are points internal to the boundary that are deemed to be on the boundary because the solution vector returns a vector that is out of bounds. To insure that there are no feasible solutions to the perturbation equation, one would have to find all the solutions at the particular point of interest in order to rule out whether or not that point lies on the boundary. An alternate approach would be to pose the above problem as a constrained optimization problem and check constraint satisfaction for each point. However, if formulating the problem in this manner is more advantageous over the numerical root finding, it may be best to proceed directly to solving the non-linear programming problem without constructing the AMS.

A second approach that is discussed in the literature is the method put forth by Abdel-Malek, Yeh, and Othman [6] that takes into account the curvature of the candidate surface and an "acceleration" term for a fictitious particle moving on the candidate surface. The acceleration term is defined to be the "difference between the

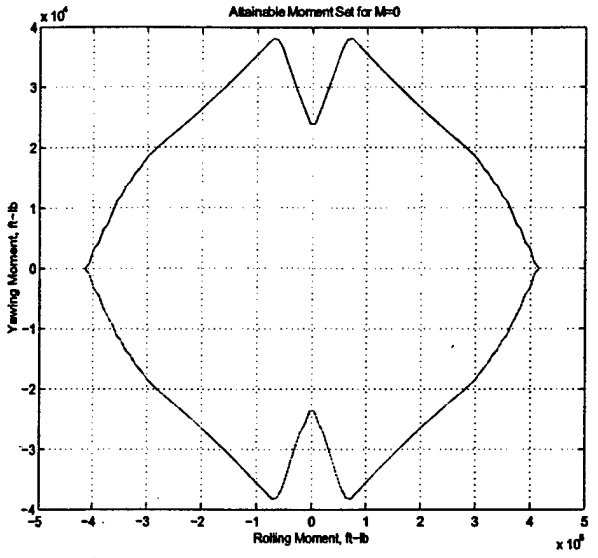

Figure 5. Achievable Yawing Moments for M=0

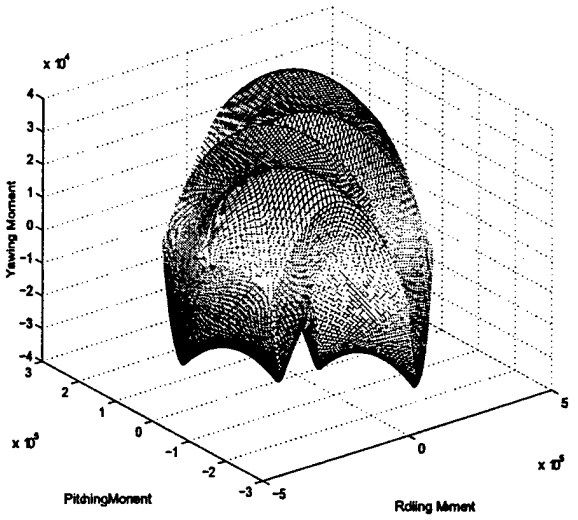

Figure 6. Non-linear Attainable Moment Set

-2489 ft-lb/deg, $K_n = -34$ ft-lb/deg^2, $C_l = K_l/2$, $C_m = K_m$, and $C_n = K_n/4$. If we fix $L = M = 0$, we get two minima with a value of $-22,950$ ft-lb. Physically, this implies that there are two different combinations of control surface deflections that will produce the minimum yawing moments while satisfying the constraints on the pitching and rolling moments. The control surface deflections corresponding to these minima are $\delta_1 = 22.5, \delta_2 = 7.5, \delta_3 = -30, \delta_4 = 0$ and $\delta_1 = -22.5, \delta_2 = -7.5, \delta_3 = 30, \delta_4 = 0$. To find the maxima, one simply changes the sign of Equation 30 the yawing moment, and repeats the steps above. In this case we get two maxima where $N = 22,950$ ft-lb.

The utility of this method is shown in Figure 5 where the AMS is shown over the range of rolling moment with pitching moment fixed to be zero. To compute the AMS, one simply needs to iterate over all values of L and M and determine the maximum and minimum values of yawing moment for each ordered pair. This approach, although exhaustive, provides an accurate estimation of the AMS. Although the approach outlined above requires that a discrete set of points in the domain is selected, and all the possible Kuhn-Tucker points constructed, it is nowhere near as computationally intensive as any of the methods discussed above, which require that each point on each candidate surface be checked for optimality.

The composite AMS is shown in Figure 6. As a comparison, Figure 7 shows the AMS generated by the linear approximation. Note first of all the difference the shapes of the two AMS's. The linear AMS predicts the correct projection onto the L-M plane, but the yawing moment is either overestimated or has the incorrect sign. The non-linear AMS provides a much more accurate representation of the aircraft's aerodynamics. Execution time was on the order of 1.2 minutes in the Matlab environment. It is expected that the algorithm's performance would increase significantly once the algorithm was implemented in another language, such as C.

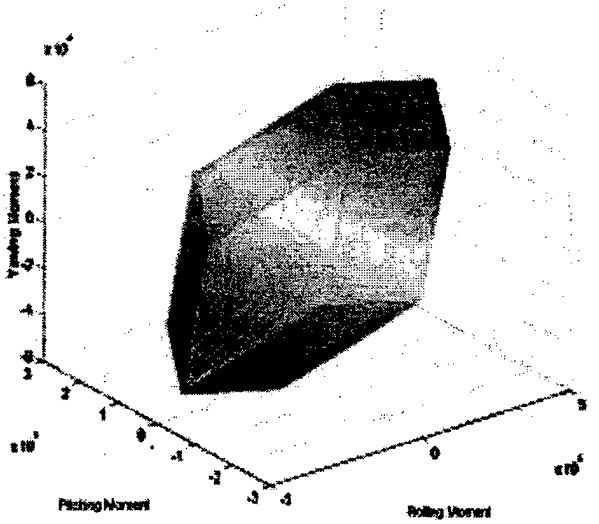

Figure 7. Linear Attainable Moment Set

4. Conclusions

A method for the determination of the attainable moment set for a class of multiple non-linear control effectors was presented. The method extends previous work that was done on the generation of the non-linear attainable moment set boundary in the planar case to the three-dimensional case, and was illustrated by considering single and multiple left-right control effector pairs. The Jacobian Rank Deficiency Criteria from Swept Vol-

ume Theory was used to construct the set of control effectors and their corresponding candidate surfaces for the boundary of the attainable moment set. The first order necessary conditions were then derived for a point to be on the boundary by considering a non-linear programming problem. An algorithm was given where the Kuhn-Tucker points for a given point in the pitch-roll plane are constructed for each control effector configuration that forms a candidate boundary. The Kuhn-Tucker points are then checked for feasibility, and the points on the boundary are the ones that maximize and minimize the objective function. This method is computationally efficient despite the fact that a large set of points in is searched since the evaluation of the Kuhn-Tucker points is straight forward and less computationally intensive than those methods which require an exhaustive search over every point on each candidate surface.

5. ACKNOWLEDGEMENTS

This work was performed while the first author held a National Research Council Research Associateship Award at the Air Force Research Laboratory.

REFERENCES

[1] M. Bodson. Evaluation of optimization methods for control allocation. *Journal of Guidance, Control, and Dynamics*, 25(4):703–711, 2002.

[2] W. Durham. Constrained control allocation: Three-moment problem. *Journal of Guidance, Control, and Dynamics*, 17(2):330–336, 1994.

[3] D.B. Doman and A.G Sparks. Concepts for constrained control allocation of mixed quadratic and linear effectors. In *Proceedings of the 2002 American Control Conference, Anchorage, AK, May 8–10, 2002.* American Automatic Control Council, 2002. Paper No. ACC02-AIAA1028.

[4] K. Abdel-Malek, D. Blackmore, and K. Joy. Swept volumes: Foundations, perspectives, and applications. *International Journal of Shape Modelling*, 21(1):1–2, 2002.

[5] K. Abdel-Malek and H Yeh. Geometric representation of the swept volume using jacobian rank deficiency conditions. *Computer Aided-Design*, 29(6):457–468, 1997.

[6] K. Abdel-Malek, H Yeh, and S. Othman. Swept volumes: Void and boundary identification. *Computer Aided-Design*, 30(13):1009–1018, 1998.